

TECHNICAL NOTE

A novel zero-dead-volume sample loading interface for microfluidic devices: flexible hydraulic reservoir (FHR)

To cite this article: Utku Hatipolu *et al* 2018 *J. Micromech. Microeng.* **28** 097001

View the [article online](#) for updates and enhancements.

Related content

- [The performance of bioinspired valveless piezoelectric micropump with respect to viscosity change](#)
Seung Chul Lee, Sunghoon Hur, Dooho Kang *et al.*
- [Minimal dead-volume connectors for microfluidics using PDMS casting techniques](#)
Chi-Han Chiou and Gwo-Bin Lee
- [Pinch-valve for lab-on-a-chip flow regulation](#)
Andrew W Browne, Kathryn E Hitchcock and Chong H Ahn



IOP | ebooks™

Bringing you innovative digital publishing with leading voices to create your essential collection of books in STEM research.

Start exploring the collection - download the first chapter of every title for free.

Technical Note

A novel zero-dead-volume sample loading interface for microfluidic devices: flexible hydraulic reservoir (FHR)

Utku Hatipoğlu¹, Barbaros Çetin¹  and Ender Yıldırım² ¹ Mechanical Engineering Department, Microfluidics & Lab-on-a-chip Research Group, İhsan Doğramacı Bilkent University, Ankara 06800, Turkey² Mechanical Engineering Department, Çankaya University, 06790 Ankara, TurkeyE-mail: barbaros.cetin@bilkent.edu.tr

Received 28 March 2018, revised 26 April 2018


Accepted for publication 8 May 2018

Published 31 May 2018

**Abstract**

Infusing minute amounts of valuable liquids such as samples to microfluidic chips by using common pumping schemes such as syringe pumps often result in an excessive dead-volume. We present a simple yet effective sample loading interface, which helps by pumping the sample to the chip by using the hydraulic pressure generated by the syringe pump. Results show that sample volumes as low as $25\mu\text{l}$ can be delivered at flow rates ranging between $10\text{--}30\mu\text{l min}^{-1}$. Maximum dead volume ratio was observed to be 3% when infusing $200\mu\text{l}$ of sample at $10\mu\text{l min}^{-1}$.

Keywords: microfluidics, syringe pump, sample loading, low-dead-volume

 Supplementary material for this article is available [online](#)

(Some figures may appear in colour only in the online journal)

1. Introduction

Microfluidics is a growing field with an impact on both diagnostic and therapeutic applications [1–5] as well as micro/nano-particle synthesis [6–8]. Generating a fluid flow is an essential ingredient for the functionality of microfluidic devices. Although different techniques such as electro-kinetic, magnetic, mechanical micro-pumps have been proposed for microfluidic applications [9, 10], owing to their simplicity and robustness, syringe pumps have been the most widely used and a viable option in most of the microfluidic research environments. Operation of a syringe pump basically relies on creating a displacement on the piston of a syringe loaded with a sample, and delivering the sample into a microfluidic device in a controlled manner in various flow-rates with an electro-mechanical system. They are compatible with nearly all syringe types available in the market. A syringe pump

is integrated with a microfluidic device through tubings. Although very low-cost macro-scale syringes and tubings are easy and convenient to use, they may create great amount of dead volume. Albeit, the implementation of micro-scale capillaries and syringes is possible, they may be expensive for a disposable set, in addition, integration and sealing may require some special care.

One big issue related to syringe pumps is that even if the piston is pushed to the very end, there are always some remaining fluid in the neck of the syringe and within the tubings (please see figure 1). Knowing the diameter (d) and the length (L) of the tube, the dead volume remaining in the tubing can be estimated as $V_{d,tube} = (\pi d^2/4)L$. The variation of the dead volume per unit length of tubing is also presented in figure 1. This dead-volume may typically be large in comparison to volume of the microchannel [11], unless a small diameter capillary tubing of very short length is used as the

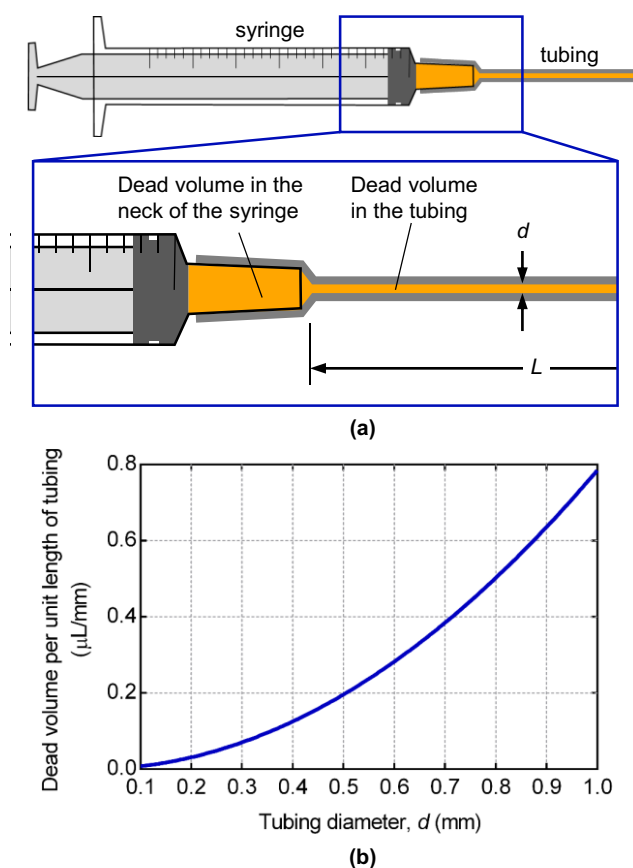


Figure 1. Schematics of (a) FHR, (b) default position and sample loading stage.

interconnect. In addition to the dead volume in the tubing, internal volume of the standard interfaces such as Luer-cone or Luer-lock at the neck of the syringe also introduces a considerable dead-volume [12] which may be as much as 25 μl for the largest piece. Although, dead volume may not be a crucial problem for many applications, it comes to prominence while working with rare and/or valuable samples, especially in biological applications or for applications like chromatography and electrophoresis where it is critical for the process performance [12].

For storage and dead-volume free delivery of minute amount of valuable samples, microfluidic reservoirs have recently been proposed as integral parts of on-chip micro-pumps [13–17]. Such designs typically comprise of closed reservoirs isolated from the rest of the microfluidic device by passive check valves. Deflecting a diaphragm on the reservoir results in the fluid pre-filled in the reservoir flow through the check valve along the microchannels. Alternative to passive check valves, integrated active valves with low dead volume are also available [18]. However, these devices require an elastic material for the diaphragm and check valves which limit the material selection, and add an extra complexity to both for fabrication and operation of a microfluidic device.

In this paper, we present a low-cost, easy-to-use, zero-dead-volume sample loading interface, what we called flexible hydraulic reservoir (FHR), which solely uses

hydraulic pressure supplied by the syringe pump for delivering the sample into a microfluidic device. The interface contains a flexible nitrile membrane that creates an interface between the dummy hydraulic fluid and (valuable) sample. Hydraulic fluid is pumped by a syringe pump to the hydraulic chamber and it creates a pressure which consequently deflects the flexible membrane. Deflected membrane creates pressure in the sample chamber which eventually delivers the sample into the microfluidic device. FHR is designed as a stand-alone device which can easily be integrated to many microfluidic devices with different architecture and configurations. It is very suitable for biomedical applications since it minimizes dead volume, it is disposable, and it enables the contamination free sample delivery.

2. Design and working principle

Figure 2 shows the schematics of the FHR and its characteristic dimensions. FHR consists of a top casing, bottom casing and nitrile membrane. In the assembly, the nitrile membrane is placed in between the top and bottom casings to create two distinct chambers. The cavity between the top casing and membrane forms the hydraulic chamber, whereas the cavity between the membrane and bottom casing forms the sample chamber. In the default position, hydraulic chamber is fully-filled with a (dummy) fluid (which can be any incompressible fluid), and the volume of the sample chamber is zero. After sample loading, hydraulic chamber shrinks as much as the volume of loaded fluid, and eventually membrane deflects towards the hydraulic chamber. Since the deflection profile is parabolic, the sample volume is always less than the hydraulic chamber volume. When the deflection is maximum (figure 2(b)), maximum sample volume becomes half of the volume of the hydraulic chamber ($V_{sample,max} = \pi D^2 h/8$).

Note that in the loaded phase, there is no positive pressure in the device (considering zero gauge pressure) therefore the risk of potential leakage is minimized. Once it is loaded, FHR is ready to be integrated to a microfluidic device. The syringe which is attached to the hydraulic chamber can be either driven by hand or a syringe pump or a pressure pump to increase the pressure of the hydraulic chamber which consequently deflects back the membrane and pushes the sample out of the FHR into the microfluidic device. Here it should be noted that the membrane deflects back to its default position, in which the volume of the sample chamber is zero, during injection (figure 2(b)). This reduces the dead-volume practically down to zero.

Working principle of the FHR is based on Pascal's Principle which defines the basic pressure distribution in a fluid. According to the law, pressure is spatially constant in a pressurized fluid. In the FHR, when the hydraulic pressure starts to increase, the fluid exerts the same force to the membrane independent from the location. This way, the pressure created by the syringe driver can be transferred to the membrane without any loss. The incompressibility of the dummy fluid and sample liquid ensures the same fluid displacement as the piston, and the same liquid displacement for the sample.

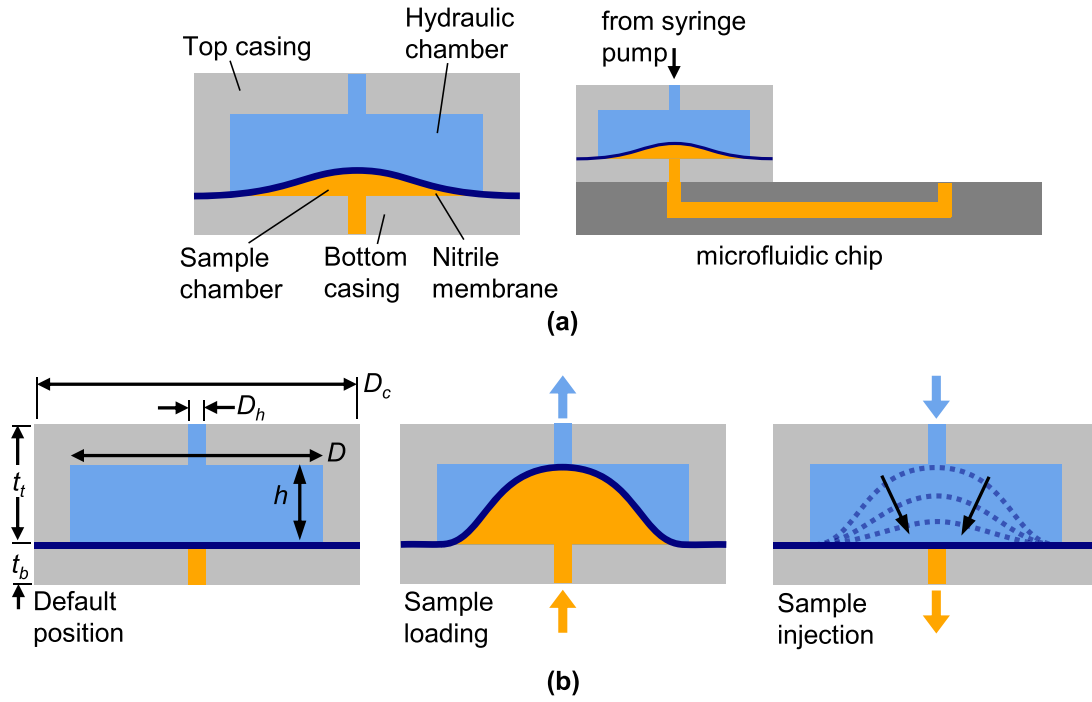


Figure 2. Schematics of (a) FHR, (b) default position, sample loading and injection stages.

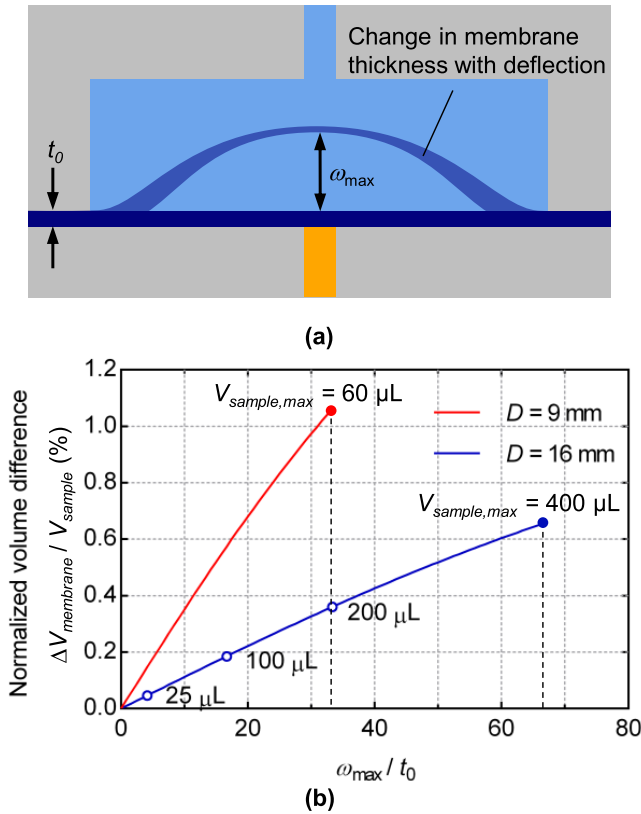


Figure 3. (a) Schematics of the deflected membrane, (b) volume change of the membrane.

When the membrane experiences a large deflection during the sample loading, its volume may change depending on the Poisson’s ratio of the membrane material (see figure 3). The change in the membrane volume may affect the infused sample

volume and also may induce some nonlinearity in the dynamic response of the FHR. The change in membrane volume is negligible in the case of nitrile which has a Poisson’s ratio of 0.45 (close to 0.5 which implies a perfectly incompressible material). However, this effect may become significant as the Poisson’s ratio decreases. For relatively low Poisson’s ratio materials the change in the thickness of membrane may be negligible which represents the worst-case scenario. For this worst-case scenario, a simple analytical model can be presented as follows [19]:

$$\omega(r) = \omega_{max} \left[1 - \left(\frac{r}{R} \right)^2 \right] \quad (1)$$

where ω_{max} is the maximum deflection of the membrane, ω is the local deflection of the membrane, R is the membrane radius ($D/2$), and t_0 is the default thickness of the membrane. The volume of the membrane can be obtained as:

$$V_{membrane} \approx 2\pi t_0 \int_0^{\omega_{max}} r(\omega) \sqrt{1 + \left(\frac{dr}{d\omega} \right)^2} d\omega \quad (2)$$

$$V_{membrane} \approx \frac{\pi t_0 R^4}{6\omega_{max}^2} \left\{ \left[1 + \left(\frac{2\omega_{max}}{R} \right)^2 \right]^{3/2} - 1 \right\}.$$

The difference between the deflected volume ($V_{membrane}$) and the initial volume (V_0) of the membrane over the sample volume loaded at this position ($V_{sample} = \pi R^2 \omega_{max} / 2$, i.e. the volume under the membrane) is plotted in figure 3 for two different chamber diameters which are fabricated in this study. The tested cases are also indicated on the figure. As seen from the figure, in the worst-case scenario, the volume change is under 1% which means the change in membrane volume is negligible for FHR.

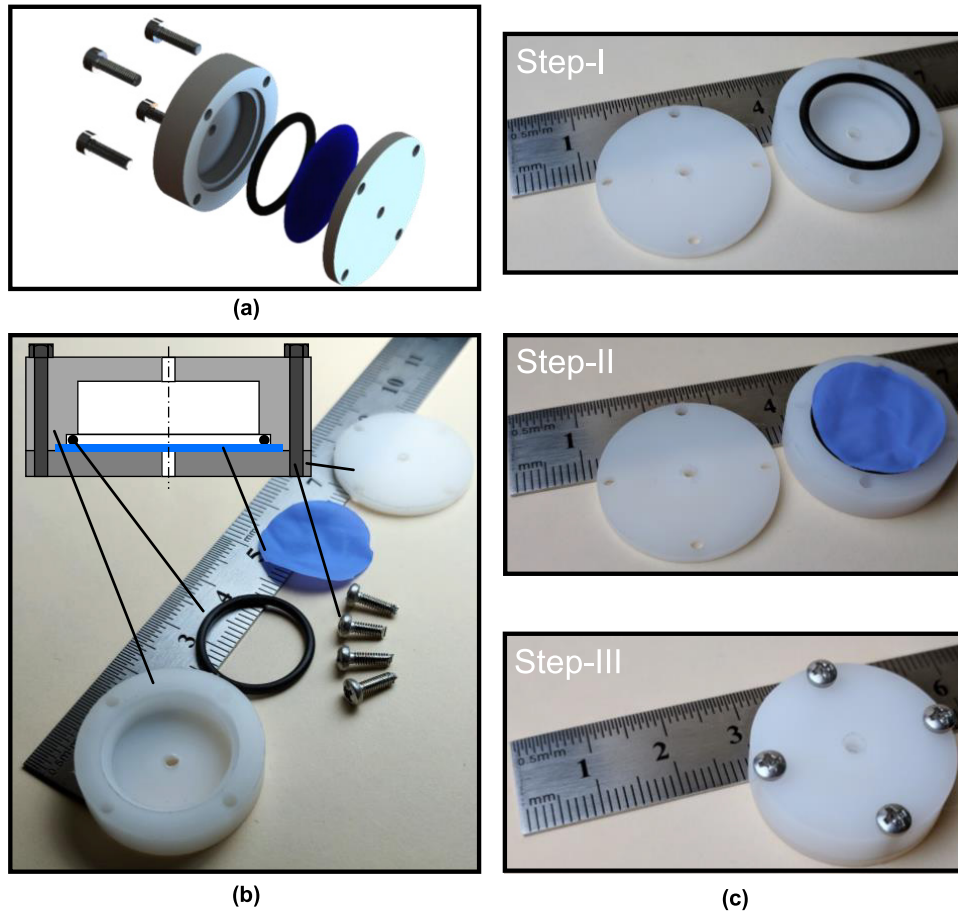


Figure 4. (a) Blow-up CAD figure, (b) photo of the components, (c) assembly process.

Table 1. Critical dimensions of the components of the FHR.

Chamber volume (μl)	Max. sample volume (μl)	D_c (mm)	D (mm)	D_h (mm)	h (mm)	t_t (mm)	t_b (mm)
800	400	25.0	16.0	2.0	4.0	6.0	2.0
120	60	17.0	9.0	2.0	2.0	4.0	2.0

3. Materials and methods

Figure 4 shows the components of the FHR and the assembly process. The blow-up CAD figure and the photo of the components are presented in figures 4(a) and (b), respectively. Critical dimensions of the components of the FHR are identified in table 1. Top and bottom casings were machined from cylindrical polyimide stock of diameter 25 mm obtained from local vendor by using a manual lathe (Opti D320 \times 920 lathe, Optimum Maschinen Germany). The volume of the resulting hydraulic chamber in the top casing was 800 μl (with a maximum sample volume of 400 μl). After creating the internal features on the top casing, the hole for connecting the tubing from the syringe was drilled. The bottom casing, which is simply in the form of a disk, was also drilled to create the hole for tubing. After machining, top and bottom casings were aligned and holes for assembly were drilled. Following the machining and drilling, to prevent leakage of the working fluid or the hydraulic fluid from one casing to the other, regular O-ring was placed in the seat on the top casing (figure 4(c),

Step-I). Since the O-ring resides in the top casing, it would not be in contact with the sample during operation, thus preventing any contamination. Then, a circular diaphragm from a nitrile sheet was cut to the same diameter with the casings and placed on the top casing (figure 4(c), Step-II). Nitrile sheet of thickness 0.06 mm was simply cut out of a nitrile examination glove again supplied from a local vendor. Stack of top casing, bottom casing, and nitrile diaphragm placed in between was assembled by using M2 bolts (figure 4(c), Step-III).

For characterization of FHR, flow of the sample was calibrated against that of the hydraulic fluid infused by a syringe pump (NE1002X, New Era Pump Systems). Water was used as the hydraulic fluid while a fluorescent dye was used as the sample. To load the dye in the sample chamber, tip of the bottom casing was immersed into the dye and the piston of the syringe was withdrawn to deflect the nitrile membrane against the top casing thus creating a negative gauge pressure in the sample chamber. Negative pressure draws the sample in the sample chamber. The volume drawn in the sample chamber was controlled by setting the withdrawn

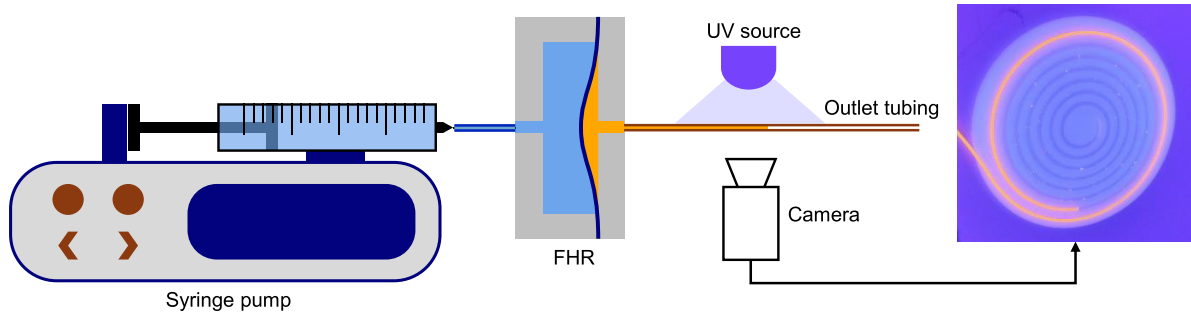


Figure 5. Schematics of the experimental set-up.

volume on the syringe pump. After loading the sample, sufficiently long tygon tubing wound in a spiral shaped holder was connected to the outlet of the bottom casing. During the tests, hydraulic fluid was infused at a constant flow rate by using a syringe pump. Meanwhile, displacement of the sample in the outlet tubing was observed by capturing a video sequence until the liquid in the sample chamber is completely delivered. Total volume of the sample delivered was calculated by counting the pixels at each frame. To improve the contrast and the quality of image processing, the outlet tubing was illuminated by UV light. Figure 5 shows the schematics of the experimental set-up. Following the experiments, the frames captured were firstly converted to binary images. A proper threshold value was defined by considering the intensity of the fluorescent dye such that only the regions with fluorescent dye remained white. Erosion method was used to cancel the noise in the binary images. Eroded binary images are then calibrated to translate the pixel size to a physical length scale. After calibration, total area of the white pixels, which represents the distance travelled by the fluorescent dye in the tubing, were measured. Measured value was multiplied by the cross-section area of the tubing to get the total volume.

4. Discussion and concluding remarks

The same FHR was tested at different flow rates (**Case-I:** $10\mu\text{l min}^{-1}$, **Case-II:** $20\mu\text{l min}^{-1}$, and **Case-III:** $30\mu\text{l min}^{-1}$). Each case was tested with different volumes of sample (25, 100, and $200\mu\text{l}$) for five times. Before each case, an experiment was conducted without FHR as a reference case. Figure 6 presents the test results. The results show that flow rate of the sample remains almost constant and equal to the flow rate of the hydraulic fluid, even when delivering very low volumes across a range of flow rates, which proves the flexibility of the design. On the other hand, it can be seen that total volume deviates slightly downwards from the reference line as the sample is completely delivered. The amount of deviation is an indicator of the dead-volume of the particular FHR. For each case, the difference between the total volume dispensed in for the reference case and the total volume dispensed by using the FHR rate at the end of the cycle was calculated and divided by the total reference volume. Greatest deviation was observed when delivering $200\mu\text{l}$ sample at $10\mu\text{l min}^{-1}$ (figure 6(a)). In this case, the ratio of

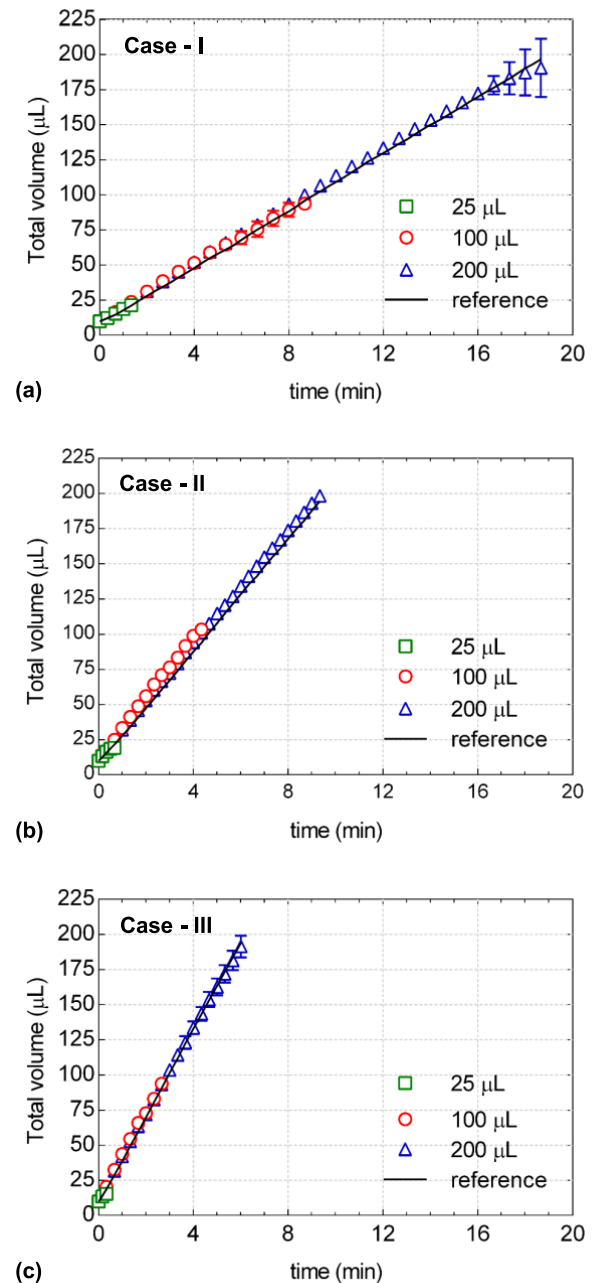


Figure 6. Test results for (a) **Case-I:** $10\mu\text{l min}^{-1}$, (b) **Case-II:** $20\mu\text{l min}^{-1}$, (c) **Case-III:** $30\mu\text{l min}^{-1}$. Error bars represent the standard error of total volume measured in five repeated experiments. Reference line represents the volume dispensed when there is no FHR, i.e. the spiral channel is directly connected to the syringe pump.

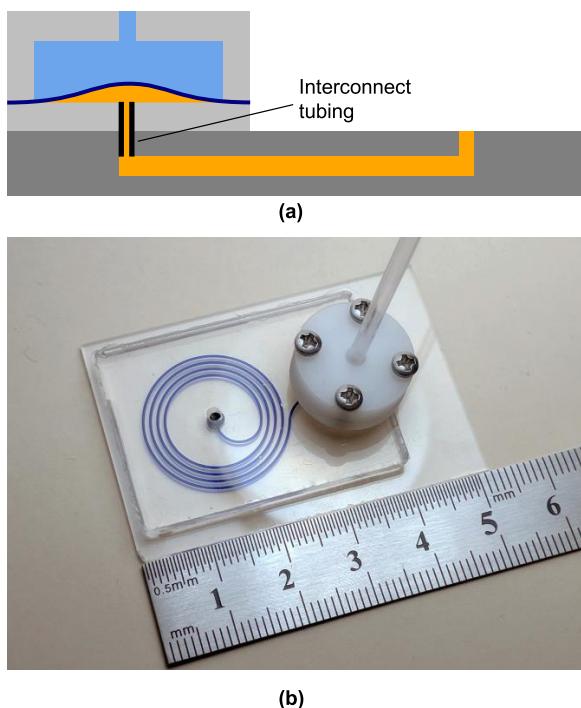


Figure 7. Integration onto a microfluidic chip: (a) Schematics, (b) photo of FHR with a chamber volume of $120\mu\text{l}$.

the dead volume to the total sample volume was calculated as 3%. The current hydraulic chamber was $800\mu\text{l}$ with a maximum sample volume of $400\mu\text{l}$. A hydraulic chamber with a smaller volume would decrease the dead volume as well as the deviation even for smaller volumetric flow rates. In this sense, FHR is quite flexible, and can be designed according to the need of a particular application.

For the experiments, FHR was loaded by inserting it into the test liquid. However, when working with valuable samples, this loading scheme may not be feasible. Different loading strategies can be implemented to load valuable samples. One possible alternative of loading the sample is using conventional pipette (please see supplementary figure S1 (stacks.iop.org/JMM/28/097001/mmedia)) which would also provide precise control of the sample volume.

Figure 7 shows an FHR with a smaller chamber volume ($120\mu\text{l}$ with a maximum sample volume of $60\mu\text{l}$) mounted on a microfluidic chip. Minimum chamber volume is limited by the machining capabilities. The chamber can be fabricated with a hydraulic chamber volume of $50\text{--}1000\mu\text{l}$ without any major problem with conventional CNC machining. Depending on the capability of the syringe pump, flow rates between $0.5\text{--}500\mu\text{l min}^{-1}$ can be implemented. If the microfluidic device has several stations for the analysis, and even the volume remaining inside the microfluidic channel network is important, the sample chamber of FHR can be preloaded with a certain amount of immiscible fluid which will push all the sample out of the microchannel network towards the exit reservoir and enable the processing of the entire sample.

The proposed sample loading interface is very user-friendly, inexpensive and has a flexible design. It can be implemented

with a syringe pump as well as a pressure pump which are available in almost every microfluidics research environment. Different materials can be used as top and bottom casings of the FHR. In the case of thermoplastics, thermal [20, 21], ultrasonic [20, 22] or adhesive bonding can be preferred in the assembly process instead of using bolts. Considering the fabrication of casings of an FHR, 3D printing can be an alternative option. However special care needs to be taken to prevent the leakage of both fluids from the FHR structure due to possible incomplete fusion of layers especially in fused deposition modeling [23].

In summary, we believe FHR will be a very convenient and useful tool for microfluidics research and microfluidic device development. Furthermore, it can also be introduced as a very inexpensive disposable set in a commercial microfluidic product to serve as an interface between the fluid pumping equipment and microfluidic chip. Further development and optimization of the FHR rely on the investigation of the dynamic response of the system. Fluid-solid interaction based computational modeling and experimental investigation of the dynamic response under different sample loading conditions need to be further explored.

ORCID iDs

Barbaros Çetin  <https://orcid.org/0000-0001-9824-4000>
Ender Yıldırım  <https://orcid.org/0000-0002-7969-2243>

References

- [1] Dittrich P S and Manz A 2006 Lab-on-a-chip: microfluidics in drug discovery *Nat. Rev. Drug Discovery* **5** 210–8
- [2] Sackmann E K, Fulton A L and Beebe D J 2014 The present and future role of microfluidics in biomedical research *Nature* **507**
- [3] Schneider G 2018 Automating drug discovery *Nat. Rev. Drug Discovery* **17** 97–113
- [4] Yager P, Edwards T, Fu E, Helton K, Nelson K, Tam M R and Weigl B H 2006 Microfluidic diagnostic technologies for global public health *Nature* **442** 412–8
- [5] Çetin B, Özer M B and Solmaz M E 2014 Microfluidic bio-particle manipulation for biotechnology *Biochem. Eng. J.* **92** 63–82
- [6] Dendukuri D, Tsoi K, Hatton T A and Doyle P S 2005 Controlled synthesis of nonspherical microparticles using microfluidics *Langmuir* **21** 2113–6
- [7] Dendukuri D, Pregibon D C, Collins J, Hatton T A and Doyle P S 2006 Continuous-flow lithography for high-throughput microparticle synthesis *Nat. Mater.* **5** 365–9
- [8] Phillips T W, Lignos I G, Maceiczuk R M, DeMello A J and DeMello J C 2014 Nanocrystal synthesis in microfluidic reactors: where next? *Lab Chip* **14** 3172
- [9] Laser D J and Santiago J G 2004 A review of micropumps *J. Micromech. Microeng.* **14** R35–64
- [10] Iverson B D and Garimella S V 2008 Recent advances in microscale pumping technologies: a review and evaluation *Microfluidics Nanofluidics* **5** 145–74
- [11] Futterer C, Minc N, Bormuth V, Codarbox J-H, Laval P, Rossier J and Viovy J-L 2004 Injection and flow control system for microchannels *Lab Chip* **4** 351–6

- [12] Becker H 2010 One size fits all? *Lab Chip* **10** 1894–7
- [13] Gong M M, MacDonald B D, Vu Nguyen T and Sinton D 2012 Hand-powered microfluidics: a membrane pump with a patient-to-chip syringe interface *Biomicrofluidics* **6** 044102
- [14] Weibel D B, Siegel A C, Lee A, George A H and Whitesides G M 2007 Pumping fluids in microfluidic systems using the elastic deformation of poly(dimethylsiloxane) *Lab Chip* **7** 1832
- [15] Zhou P, Young L and Chen Z 2010 Weak solvent based chip lamination and characterization of on-chip valve and pump *Biomed. Microdevices* **12** 821–32
- [16] Chen X, Shen J, Hu Z and Huo X 2016 Manufacturing methods and applications of membranes in microfluidics *Biomed. Microdevices* **18** 104
- [17] Guevara-Pantoja P A, Jiménez-Valdés R J, Garcia-Cordero J L and Caballero-Robledo G A 2018 Pressure-actuated monolithic acrylic microfluidic valves and pumps *Lab Chip* **18** 662–9
- [18] Godino N, del Campo F J, Munoz F X, Hansen M F, Kutter J P and Snakenborg D 2010 Integration of a zero dead-volume pdms rotary switch valve in a miniaturised (bio)electroanalytical system *Lab Chip* **10** 1841–7
- [19] Schomburg W K 2011 *Introduction to Microsystem Design* RWTH edn (Berlin: Springer) pp 29–52
- [20] Temiz Y, Lovchik R D, Kaigala G V and Delamarche E 2015 Lab-on-a-chip devices: how to close and plug the lab? *Microelectron. Eng.* **132** 156–75
- [21] Chen X, Shen J and Zhou M 2016 Rapid fabrication of a four-layer pmma-based microfluidic chip using CO₂-laser micromachining and thermal bonding *J. Micromech. Microeng.* **26** 107001
- [22] Becker H, Mikrotechnik J and Jena M 2000 Polymer microfabrication methods for microfluidic analytical applications *Electrophoresis* **21** 12–26
- [23] Bhattacharjee N, Urrios A, Kang S and Folch A 2016 The upcoming 3D-printing revolution in microfluidics *Lab Chip* **16** 1720–42